Time-domain constraints for passive materials: The Brendel-Bormann model revisited

Sven Nordebo [*]
Department of Physics and Electrical Engineering, Linnæus University, 351 95 Växjö, Sweden

Martin Štumpf [†]
Lerch Laboratory of EM Research, Department of Radio Electronics, FEEC, Brno University of Technology, Technická 3082/12, 616 00 Brno, The Czech Republic
and Department of Computer Science, Electrical and Space Engineering, EISLAB, Luleå University of Technology, 971 87 Luleå, Sweden

(Received 7 February 2024; revised 16 May 2024; accepted 1 July 2024; published 9 July 2024)

This paper presents a systematic approach to derive physical bounds for passive systems, or equivalently for positive real (PR) functions, directly in the time-domain (TD). As a generic, canonical example we explore the TD dielectric response of a passive material. We will furthermore revisit the theoretical foundation regarding the Brendel-Bormann (BB) oscillator model which is reportedly very suitable for the modeling of thin metallic films in high-speed optoelectronic devices. To this end, an important result here is to re-establish the physical realizability of the BB model by showing that it represents a passive and causal system. The theory is based on Cauer's representation of an arbitrary PR function together with associated sum rules (moments of the measure) and exploits the unilateral Laplace transform to derive rigorous bounds on the TD response of a passive system. Similar bounds have recently been reported for more general casual systems with other *a priori* assumptions. To this end, it is important to note here that the existence of useful sum rules and related physical bounds rely heavily on an assumption about the PR functions having a low- or high-frequency asymptotic expansion at least of odd order 1. As a particular numerical example, we consider here the electric susceptibility of gold (Au) which is commonly modeled by well established Drude or BB models. Explicit physical bounds are given as well as an efficient fast-Fourier transform -based numerical procedure to compute the TD impulse response associated with the nonrational BB model.

DOI: 10.1103/PhysRevB.110.024307

I. INTRODUCTION

It is well known that the Kramers-Kronig relations limit the dispersive behavior of a linear, time-invariant and causal system [1]. The additional assumption of passivity may furthermore imply additional physical limitations on what is possible to realize in a finite bandwidth. More precisely, we refer here to immittance passivity, which by itself implies that the system is causal [2]. Classical examples are the bounds on broadband matching using lossless networks that were derived by Fano [3]. More recent examples are the physical bounds that have been obtained concerning radar absorbers, high-impedance surfaces, passive metamaterials, broadband quasistatic cloaking, scattering, antennas, reflection coefficients, waveguides and periodic structures, only to mention a few. A survey of recent examples and applications in electromagnetics is given in Ref. [4].

The immittance passive systems can be completely characterized by positive real (PR) functions (analytic functions mapping the right half-plane into itself), or equivalently, by the so-called (symmetric) Herglotz functions (analytic functions mapping the upper half-plane into itself), also known as Nevanlinna or Herglotz-Nevanlinna functions, cf., e.g., Refs. [1,2,5–7]. Provided that a PR function has some odd ordered low- and/or high-frequency asymptotic expansion at least of order 1, a partial knowledge about the expansion coefficients can then sometimes be used to derive sum rules (integral identities) which may have a useful physical interpretation. Physical bounds can then been obtained by restricting an integral to a finite frequency interval and hence bounding it from above by the corresponding sum rule (moments of a positive measure), see e.g., Refs. [4,8]. However, there can still be many interesting applications to explore and what is still missing is an investigation about the physical limitations of a passive system that can be formulated directly in the time-domain (TD).

A new approach to derive physical bounds in the TD has recently been given in Refs. [9,10]. This technique takes as its starting point the low- and high-frequency asymptotic properties of a linear, time-invariant and casual system and exploits its analytical properties to derive physical bounds directly in the TD. In particular, by exploring various subclasses of linear systems and their asymptotic properties together with some adequately chosen unipolar input pulses, it has been

[*]Contact author: sven.nordebo@lnu.se
[†]Contact author: martin.stumpf@centrum.cz; martin.stumpf@ltu.se

demonstrated how new *early-time* as well as *late-time* physical bounds on the system response can be derived. Sometimes these bounds can furthermore be combined by their common *corner time* to provide useful *all-time* bounds. The purpose of this paper is to systematically explore these ideas by assuming that the linear system is *immittance passive* and hence can be characterized by a PR function. The present approach is based on Cauer's representation [2] of an arbitrary PR function and its associated sum rules [4]. The unilateral Laplace transform is employed to obtain a theory which is directly applicable in the TD. Similar as with the TD bounds derived in Refs. [9,10], an important motivation for the derivation of TD bounds for passive systems is for their future potential to benchmark non-passive and possibly time varying systems such as with gain or active media [11,12], parity-time symmetric planar devices [13], active photonic metasurfaces [14], temporal modulations [15] or cloaking [16], only to mention a few.

Moreover, the TD physical bounds may find their applications in worst-case studies within electromagnetic compatibility (EMC) including electronic signals intelligence and EM (nuclear/lightning) pulse protection, as well as in designing high-speed electronic and photonic switching circuits, see, e.g., Refs. [17–21] for further references. As a generic, canonical example we choose here to investigate TD physical bounds on the dielectric response of a passive material and as an important case study we consider the well known Brendel-Bormann (BB) oscillator model [20]. To this end, it is an additional purpose of this paper is to re-establish the BB model as a perfectly sound physical model for the permittivity of a passive material in contrast to what has been claimed in Refs. [22,23]. The BB model was originally introduced for the modeling of thin metallic films and their response to infrared radiation with applications such as mirrors and microelectronic contacts in high-speed optoelectronic devices [20,21]. The BB model has since become highly appreciated due to its ability to accurately represent measured dielectric data from near infrared, visible, and near ultraviolet regions of the electromagnetic spectra. Hence, the model is now appearing in various applications such as modal analysis of plasmonic structures [24–26], photoluminescence modeling [27], dielectric function data sets [28] and as a model for silicon oxide thin films [29], only to mention a few. However, it has also been claimed that the BB model is unphysical as it is noncausal and asymmetric [22,23]. By using the theory of PR functions we will show in this paper that neither of these claims are true.

As particular numerical examples we will consider here the electric susceptibility of gold (Au) and give explicit bounds on its early-time impulse and step responses in terms of its plasma frequency which can be derived from well established Drude [30] and BB models [21]. To this end, it is noted that the TD bounds quantify the fact that a metal (in particular a Drude or a BB material) behaves asymptotically as a conductor at low frequencies (late times) and increasingly as a lossless dielectric at higher frequencies (early times). An efficient fast-Fourier transform (FFT)-based numerical procedure is finally developed in order to validate the TD impulse response of the BB model against its physical bounds. In particular, it is found that on the realistic time scales associated with switching frequencies in the intermediate infrared region, it is the Drude mechanism of the BB model that governs the early time response of the material.

The rest of the paper is organized as follows. In Appendix A is given a brief survey of the most important properties of PR functions and their associated integral identities (sum rules), which are needed here. In Appendix B we briefly discuss the connection between these integral identities and the sum rules originally formulated in quantum mechnanics. In Appendix C a detailed account is given on the physical realizability of the BB model including a discussion on the plausible causes to the misconceptions made in Refs. [22,23]. A general description of the TD bounds for PR functions which can be derived based on their associated sum rules is given in Sec. II. The theory is then specialized to the impulse and step responses of a passive dielectric material in Sec. III. The BB model, its frequency asymptotics and associated TD bounds as well as its numerical implementation in the TD is treated in detail in Sec. IV. A summary with conclusions are finally given in Sec. V.

II. TIME-DOMAIN CONSTRAINTS FOR POSITIVE REAL FUNCTIONS

Basic properties and sum rules for PR functions are given in Appendix A. Several TD constraints for PR functions can be derived based on Cauer's representation Eq. (A3) together with the sum rules Eqs. (A10) and (A11). For the cases where this is possible the corresponding bounds are rigorous due to the strict positivity of the generating measure β. The number of feasible formulations are, however restricted by the structure of the asymptotic expansions in Eqs. (A8) and (A9). Note in particular the requirement of having an *odd* expansion within the range of feasible sum rules for $n = 0, 2, 4, \ldots$. Note also that we may have different expansion orders M associated with Eqs. (A8) and (A9). Below, we will demonstrate the procedure by explicitly deriving a number of useful constraints that are associated with the minimum required asymptotic order $M = 1$. Higher order constraints can be similarly derived if the necessary *a priori* information is available.

A. Early-time bounds

We start by rewriting Cauer's representation (A3) for an arbitrary PR function as

$$p(s) = b_1 s + a_{-1} s^{-1} + \int_{\mathbb{R}\setminus\{0\}} \frac{s}{s^2 + \xi^2} \mathrm{d}\beta(\xi), \tag{1}$$

where s is the ordinary Laplace variable with $\mathrm{Re}\{s\} > 0$, $b_1 \geqslant 0$, $a_{-1} \geqslant 0$ and $\beta(\xi)$ is a positive Borel measure with growth condition given by Eqs. (A4). The inverse Laplace transform is then given by the following distribution of slow growth:

$$p(t) = b_1 \delta^{(1)}(t) + a_{-1} H(t) + H(t) \int_{\mathbb{R}\setminus\{0\}} \cos(\xi t) \mathrm{d}\beta(\xi), \tag{2}$$

where $H(t)$ is the Heaviside unit step function and $\delta^{(1)}(t)$ the first-order derivative of the Dirac delta function $\delta(t)$, see also [2, Theorem 10.5-1]. For notational convenience we let the argument of a function $f(\cdot)$ decide whether we refer to

the time domain $f(t)$ or to the Laplace domain $f(s)$, etc. It is furthermore noticed that $p(t)$ corresponds to the impulse response of an immittance passive system and is always a causal function, see also Ref. [2, Chap. 10.3].

Let us now furthermore assume that there exists an odd ordered high-frequency asymptotic expansion of order 1

$$p(s) = \begin{cases} a_{-1}s^{-1} + o(s^{-1}), & \text{as } s \hat{\to} 0 \\ b_1 s + b_{-1}s^{-1} + o(s^{-1}), & \text{as } s \hat{\to} \infty, \end{cases} \tag{3}$$

according to the definitions made in Eqs. (A8) and (A9) and where $o(\cdot)$ denotes the small ordo according to the definition made in, e.g., Ref. [31, p. 4]. We have then the following sum rule (A11) for $n = 0$

$$\int_{\mathbb{R}\setminus\{0\}} \mathrm{d}\beta(\xi) = b_{-1} - a_{-1}. \tag{4}$$

From the positivity of the measure it is concluded that $b_{-1} - a_{-1} \geqslant 0$ and where $b_{-1} = a_{-1}$ corresponds to the trivial case for which the positive measure β is different from zero on $\mathbb{R} \setminus \{0\}$ only at a set of measure zero. From Eq. (2) follows now that

$$\begin{aligned} &\pm \left(p(t) - b_1\delta^{(1)}(t) - a_{-1}H(t)\right) \\ &\quad = \pm H(t) \int_{\mathbb{R}\setminus\{0\}} \cos(\xi t)\mathrm{d}\beta(\xi) \\ &\quad \leqslant H(t) \int_{\mathbb{R}\setminus\{0\}} \mathrm{d}\beta(\xi) = (b_{-1} - a_{-1})H(t), \end{aligned} \tag{5}$$

and where the inequality should be understood in the distributional sense.

We can now derive a simple early-time bound for the response of any right-sided and unipolar input pulse shape $f(t) \geqslant 0$ for $t \geqslant 0$ directly from Eq. (5) as

$$|p(t) * f(t) - b_1\delta_t f(t) - a_{-1}\delta_t^{-1}f(t)| \leqslant (b_{-1} - a_{-1})\delta_t^{-1}f(t), \tag{6}$$

where $*$ denotes the time-domain convolution, δ_t the time derivative and

$$\delta_t^{-1}f(t) = H(t) * f(t) = \int_{0-}^{t} f(\tau)\mathrm{d}\tau, \tag{7}$$

see also Ref. [9]. Even though the bound in Eq. (6) is an all-time bound valid for all $t > 0$Â we refer to it as an early-time bound as it is generally most accurate asymptotically as $t \to 0+$. It is noted that the inequality in Eq. (5) is preserved under the convolution as the pulse shape $f(t)$ is assumed to be non-negative on its region of support $[0, \infty)$. It is furthermore assumed that $f(t)$ is generally a distribution of slow growth and that its unilateral Laplace transform $f(s)$ exists. To this end, the operator δ_t^{-n} will denote the time-domain integrator of order n corresponding to a multiplication with s^{-n} in the Laplace domain. It should also be noted that the presence of the distributions $\delta^{(1)}(t)$ and $H(t)$ inside the left-hand side parenthesis in Eq. (5) actually means the *removal* of these distributions from the left-hand side expression.

The expression (6) generally provides an early-time (all-time) bound given that $p(t) * f(t)$ is unknown but $f(t)$, $\delta_t f(t)$ and $\delta_t^{-1}f(t)$ are known as well as the coefficients a_{-1}, b_{-1} and b_1. It is noted that the case with $b_{-1} = a_{-1}$ is the trivial case when $p(s) = b_1 s + a_{-1}s^{-1}$ and $p(t) * f(t) = b_1\delta_t f(t) + a_{-1}\delta_t^{-1}f(t)$. In case we do not know $f(t)$, $\delta_t f(t)$ and $\delta_t^{-1}f(t)$ in explicit mathematical form but can estimate the integral $B = \int_0^\infty f(\tau)\mathrm{d}\tau$, we can exploit the inequality $\delta_t^{-1}f(t) \leqslant B$ extended directly on the right-hand side of Eq. (6) to obtain a constant all-time bound valid for all $t > 0$, see also Ref. [9].

In the case with the dielectric responses studied in this paper, a first obvious choice is to let $f(t)$ in Eq. (6) be the step function $H(t)$, and consequently

$$\begin{aligned} f(s) = \frac{1}{s} \quad & f(t) = H(t), \\ sf(s) = 1 \quad & \delta_t f(t) = \delta(t), \\ \frac{1}{s}f(s) = \frac{1}{s^2} \quad & \delta_t^{-1}f(t) = tH(t). \end{aligned} \tag{8}$$

This will be used here to obtain early-time bounds directly on the dielectric susceptibility function itself. However, we will first illustrate the basic technique by studying a generalized step response of the dielectric susceptibility function. For this purpose we make the following definitions:

$$\begin{aligned} f(s) &= \frac{1/\tau}{s^2(s+1/\tau)} = \frac{\tau}{s+1/\tau} + \frac{1}{s^2} - \frac{\tau}{s}, \\ sf(s) &= \frac{1/\tau}{s(s+1/\tau)} = \frac{1}{s} - \frac{1}{s+1/\tau}, \\ \frac{1}{s}f(s) &= \frac{1/\tau}{s^3(s+1/\tau)} = \frac{\tau}{s(s+1/\tau)} + \frac{1}{s^3} - \frac{\tau}{s^2}, \end{aligned} \tag{9}$$

together with the corresponding TD expressions

$$\begin{aligned} f(t) &= (\tau \mathrm{e}^{-t/\tau} + t - \tau)H(t), \\ \delta_t f(t) &= (1 - \mathrm{e}^{-t/\tau})H(t), \\ \delta_t^{-1}f(t) &= \left(\tau^2(1 - \mathrm{e}^{-t/\tau}) + \tfrac{1}{2}t^2 - \tau t\right)H(t). \end{aligned} \tag{10}$$

Here, the generalized step function is given by $\delta_t f(t) = (1 - \mathrm{e}^{-t/\tau})H(t)$ and which is now associated with the raise time $\tau > 0$. From the partial fractions in Eq. (9) it is readily seen that the case with $\tau = 0$ is perfectly consistent with the case where $\delta_t f(t) = H(t)$ is the ordinary unit step function, $f(t) = tH(t)$ is the ramp and $\delta_t^{-1}f(t) = \frac{1}{2}t^2H(t)$.

B. Late-time bounds

The next useful possibility of exploiting sum rules for PR functions comes from the ramp response

$$\frac{1}{s^2}p(s) = b_1 s^{-1} + a_{-1}s^{-3} + \int_{\mathbb{R}\setminus\{0\}} \frac{1}{s(s^2+\xi^2)}\mathrm{d}\beta(\xi), \tag{11}$$

yielding the following inverse Laplace transform:

$$\begin{aligned} \delta_t^{-2}p(t) &= b_1 H(t) + a_{-1}\frac{1}{2}t^2H(t) \\ &\quad + H(t)\int_{\mathbb{R}\setminus\{0\}} \frac{1}{\xi^2}(1 - \cos(\xi t))\mathrm{d}\beta(\xi). \end{aligned} \tag{12}$$

Let us now furthermore assume that there exists an odd ordered low-frequency asymptotic expansion of order 1

$$p(s) = \begin{cases} a_{-1}s^{-1} + a_1 s + o(s), & \text{as } s \hat{\to} 0 \\ b_1 s + o(s), & \text{as } s \hat{\to} \infty, \end{cases} \tag{13}$$

we have then the following sum rule (A10) for $n = 2$:

$$\int_{\mathbb{R}\setminus\{0\}} \frac{\mathrm{d}\beta(\xi)}{\xi^2} = a_1 - b_1. \tag{14}$$

From the positivity of the measure it is concluded that $a_1 - b_1 \geqslant 0$ and where $a_1 = b_1$ corresponds to the trivial case for which the positive measure β is different from zero on $\mathbb{R} \setminus \{0\}$ only at a set of measure zero. From Eq. (12) follows now that

$$\begin{aligned} &\pm\left(\delta_t^{-2}p(t) - b_1 H(t) - a_{-1}\frac{1}{2}t^2 H(t)\right) \\ &\quad = \pm H(t)\int_{\mathbb{R}\setminus\{0\}} \frac{1}{\xi^2}(1-\cos(\xi t))\mathrm{d}\beta(\xi) \\ &\quad \leqslant H(t)\int_{\mathbb{R}\setminus\{0\}} \frac{1}{\xi^2} 2\mathrm{d}\beta(\xi) = 2(a_1 - b_1)H(t), \end{aligned} \tag{15}$$

and hence

$$\left|\delta_t^{-2}p(t) - b_1 H(t) - a_{-1}\tfrac{1}{2}t^2 H(t)\right| \leqslant 2(a_1 - b_1)H(t). \tag{16}$$

It is noted that the trivial case with $a_1 = b_1$ implies that $p(s) = b_1 s + a_{-1}s^{-1}$ and $\delta_t^{-2}p(t) = b_1 H(t) + a_{-1}\frac{1}{2}t^2 H(t)$.

Finally, by assuming that there exists both a low-frequency as well as a high-frequency odd asymptotic expansion of order 1

$$p(s) = \begin{cases} a_{-1}s^{-1} + a_1 s + o(s), & \text{as } s \hat{\to} 0, \\ b_1 s + b_{-1}s^{-1} + o(s^{-1}), & \text{as } s \hat{\to} \infty, \end{cases} \tag{17}$$

we can then combine the result (6) using the ramp $f(t) = tH(t)$ for which $f(s) = s^{-2}$ [$\tau = 0$ in Eqs. (9) and(10)] together with Eq. (16) to get the more general all-time bound

$$\begin{aligned} &\left|\delta_t^{-2}p(t) - b_1 H(t) - a_{-1}\tfrac{1}{2}t^2 H(t)\right| \\ &\quad \leqslant \begin{cases} (b_{-1} - a_{-1})\frac{1}{2}t^2 H(t) & t \leqslant t_{\mathrm{c}}, \\ 2(a_1 - b_1)H(t) & t \geqslant t_{\mathrm{c}}, \end{cases} \end{aligned} \tag{18}$$

and where the *corner time* t_{c} is given by

$$t_{\mathrm{c}} = \sqrt{\frac{4(a_1 - b_1)}{b_{-1} - a_{-1}}}, \tag{19}$$

cf., also Ref. [9].

III. RESPONSE OF A DIELECTRIC MATERIAL

It is well known that the normalized dielectric constant (permittivity function) $\epsilon(s)$ of a passive material is associated with the positive real function

$$p(s) = s\epsilon(s) \tag{20}$$

so that $p(t) = \delta_t \epsilon(t)$, cf., Refs. [4,32]. Thus, provided that the asymptotics (17) are valid and the bounds in Eq. (18) are applicable, we obtain an interesting TD bound for the unit step response of a dielectric material involving a quadratic early-time bound and a constant late-time bound as

$$\begin{aligned} &\left|\epsilon(t) * H(t) - b_1 H(t) - a_{-1}\tfrac{1}{2}t^2 H(t)\right| \\ &\quad \leqslant \begin{cases} (b_{-1} - a_{-1})\frac{1}{2}t^2 H(t) & t \leqslant t_{\mathrm{c}}, \\ 2(a_1 - b_1)H(t) & t \geqslant t_{\mathrm{c}}, \end{cases} \end{aligned} \tag{21}$$

where we have used that $\delta_t^{-2}p(t) = \delta_t^{-1}\epsilon(t) = \epsilon(t) * H(t)$ and where the corner time is given by Eq. (19).

Given that it is only the high-frequency asymptotics (3) that can be confirmed we can only refer to the following early-time bound:

$$\begin{aligned} &\left|\epsilon(t) * H(t) - b_1 H(t) - a_{-1}\tfrac{1}{2}t^2 H(t)\right| \\ &\quad \leqslant (b_{-1} - a_{-1})\tfrac{1}{2}t^2 H(t), \end{aligned} \tag{22}$$

but which is valid for all t and asymptotically accurate as $t \to 0+$. However, in this case we may also incorporate the more general bound (6) with $f(t)$ defined by Eqs. (9) and (10) yielding

$$\begin{aligned} &\left|\epsilon(t) * \delta_t f(t) - b_1 \delta_t f(t) - a_{-1}\delta_t^{-1} f(t)\right| \\ &\quad \leqslant (b_{-1} - a_{-1})\delta_t^{-1} f(t), \end{aligned} \tag{23}$$

where $\delta_t f(t) = (1 - \mathrm{e}^{-t/\tau})H(t)$ is the generalized step function with raise time τ and $\delta_t^{-1} f(t) = (\tau^2(1 - \mathrm{e}^{-t/\tau}) + \frac{1}{2}t^2 - \tau t)H(t)$.

Except for the step response of a dielectric material we may also be interested in bounding the susceptibility function itself. For this purpose we will now assume that $a_{-1} = 0$ and write $b_1 = \epsilon_\infty = \lim_{s\to\infty}\epsilon(s)$, and define the susceptibility function as

$$\chi(s) = \epsilon(s) - \epsilon_\infty. \tag{24}$$

By using $f(s) = \frac{1}{s}$ as in Eq. (8) together with $p(s) = s\epsilon(s)$, the early-time bound (6) then becomes

$$|\chi(t)| = |\epsilon(t) - \epsilon_\infty \delta(t)| \leqslant b_{-1} t H(t). \tag{25}$$

For a conducting material it can furthermore be assumed that

$$\epsilon(s) = \frac{\varsigma}{\epsilon_0 s} + o\left(\frac{1}{s}\right), \tag{26}$$

where ς is the static conductivity of the material and ϵ_0 the permittivity of free space (vacuum). Evidently, the static conductivity can also be defined as

$$\varsigma = \epsilon_0 \lim_{s\to 0} s\chi(s) = \epsilon_0 \lim_{t\to+\infty} \chi(t), \tag{27}$$

where the last equality is due to the final value theorem of the Laplace transform. It should be noted that the susceptibility function $\chi(t)$ is also the slope of the error function associated with the step response in Eq. (22) when $a_{-1} = 0$, i.e.,

$$\chi(t) = \delta_t(\epsilon(t) * H(t) - b_1 H(t)). \tag{28}$$

Let us finally make a physical interpretation of Eq. (25) together with Eq. (27) by defining the (corner) *time of no conduction* as

$$t_{\mathrm{nc}} = \frac{\varsigma}{\epsilon_0 b_{-1}}. \tag{29}$$

Hence, t_{nc} is the initial duration of time where the material does not behave as a conductor, i.e., $\epsilon_0\chi(t) < \varsigma$ for $t < t_{\mathrm{nc}}$.

It should be noted, however, that $t < t_{\rm nc}$ is merely a sufficient condition for no conduction, while the actual (practical) time of no conduction may be much larger.

Any passive conduction model must satisfy the bounds described above. For the standard Drude model the behavior of $\chi(t)$ at small times is trivial and the bound given by (29) can be considered to be tight in a well defined sense. However, for a non-rational model such as the BB model we will need a computational procedure such as the FFT to investigate the precise behavior of $\chi(t)$ at early times. This will be described in Sec. IV B below.

Let us now investigate the asymptotic properties of the standard Lorentz and Drude dielectric models in view of the bounds given by Eqs. (21), (22), and (23). The same physical bounds are then valid for all passive materials sharing the same first order asymptotics as the standard model under consideration.

A. Lorentz model

The Lorentz model is commonly used to model the dielectric response of solids and gases with bound charges, and is given by

$$\epsilon(s) = \epsilon_\infty + \frac{\omega_{\rm p}^2}{s^2 + s\nu + \omega_0^2}, \tag{30}$$

where $\epsilon_\infty > 0$ is the optical response, $\omega_{\rm p} > 0$ the plasma frequency, $\omega_0 > 0$ the resonance frequency and $\nu \geqslant 0$ the collision frequency. The case with $\omega_0 = 0$ gives the Drude model which is treated below. The corresponding TD impulse response and unit step response for an underdamped system where $\omega_0 > \nu/2$ are given by

$$\begin{aligned}\epsilon(t) &= \epsilon_\infty \delta(t) + \frac{\omega_{\rm p}^2}{\nu_0} {\rm e}^{-\nu t/2} \sin(\nu_0 t) H(t),\\ \epsilon(t) * H(t) &= \epsilon_\infty H(t) + \frac{\omega_{\rm p}^2}{\omega_0^2}\Bigg(1 - {\rm e}^{-\nu t/2}\Bigg(\cos(\nu_0 t)\\ &\quad + \frac{\nu}{2\nu_0}\sin(\nu_0 t)\Bigg)\Bigg) H(t),\end{aligned} \tag{31}$$

where $\nu_0 = \sqrt{\omega_0^2 - \nu^2/4} > 0$. The corresponding PR function and its first-order asymptotics are given by

$$\begin{aligned} p(s) &= s\epsilon_\infty + \frac{s\omega_{\rm p}^2}{s^2 + s\nu + \omega_0^2}\\ &= \begin{cases} \epsilon_{\rm s} s + o(s) & \text{as } s \hat{\to} 0,\\ \epsilon_\infty s + \omega_{\rm p}^2 s^{-1} + o(s^{-1}) & \text{as } s \hat{\to} \infty, \end{cases}\end{aligned} \tag{32}$$

where $\epsilon_{\rm s} = \epsilon_\infty + \omega_{\rm p}^2/\omega_0^2$ is the static permittivity. We can see that the requirements given by Eq. (17) are satisfied here with

$$\begin{aligned} a_{-1} &= 0 \quad a_1 = \epsilon_{\rm s},\\ b_1 &= \epsilon_\infty \quad b_{-1} = \omega_{\rm p}^2. \end{aligned} \tag{33}$$

It is also noticed that the first-order asymptotic parameters above are independent of the loss parameter ν and where $0 \leqslant \nu < 2\omega_0$.

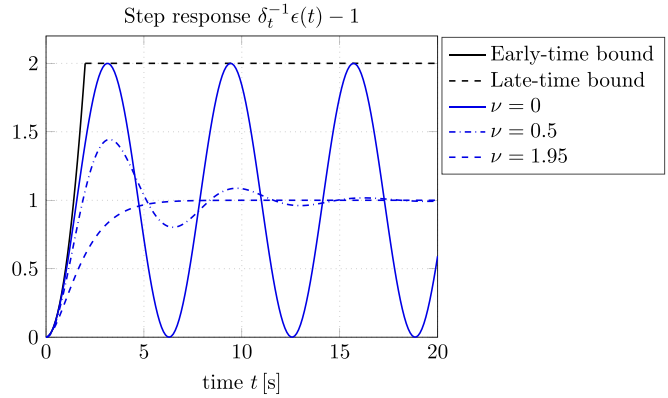

FIG. 1. Early- and late-time bounds for the unit step response of a dielectric constant with first order asymptotics given by Eq. (32) and a comparison with the actual response of the Lorentz model (31) with $\epsilon_\infty = 1$, $\omega_0 = \omega_{\rm p} = 1$ and $\nu \in \{0, 0.5, 1.95\}$. The bounds are in black color and the Lorentz responses are in blue color.

We may now consider a general passive dielectric material with the same first order asymptotics as in Eq. (32) and conclude that the bound (21) is valid. The bound is given here explicitly as

$$|\epsilon(t) * H(t) - \epsilon_\infty H(t)| \leqslant \begin{cases} \omega_{\rm p}^2 \frac{1}{2} t^2 H(t) & t \leqslant t_{\rm c},\\ 2(\epsilon_{\rm s} - \epsilon_\infty) H(t) & t \geqslant t_{\rm c}, \end{cases} \tag{34}$$

and where the corner time Eq. (19) is given by

$$t_{\rm c} = \sqrt{\frac{4(\epsilon_{\rm s} - \epsilon_\infty)}{\omega_{\rm p}^2}} = \sqrt{\frac{4\omega_{\rm p}^2/\omega_0^2}{\omega_{\rm p}^2}} = \frac{2}{\omega_0}. \tag{35}$$

A numerical example is given in Fig. 1. The Lorentz model is implemented here with $\epsilon_\infty = 1$, $\omega_0 = \omega_{\rm p} = 1$ and $0 \leqslant \nu < 2$.

It is noted that the bound is tight in the loss-less case when $\nu = 0$. When losses are nonzero and $\nu > 0$, we can see that $|\epsilon(t) * H(t) - \epsilon_\infty H(t)| \to \epsilon_{\rm s} - \epsilon_\infty = \omega_{\rm p}^2/\omega_0^2$ as $t \to \infty$ in accordance with the final value theorem $\lim_{t\to\infty} \delta_t^{-1}\epsilon(t) = \lim_{s\to 0} \epsilon(s) = \epsilon_{\rm s}$ where $\epsilon_{\rm s}$ is the static permittivity. Obviously, a positive combination of multiple resonances can be treated similarly. It is also interesting to observe that the squared plasma frequency $\omega_{\rm p}^2$ could potentially be determined from accurate measurements of the early-time asymptotic quadratic response as of Eq. (34) for $t \ll t_{\rm c}$.

B. Drude model

The Drude model is used to model the conduction of charges in metals and is a special case of the Lorentz model with resonance frequency $\omega_0 = 0$. Here

$$\epsilon(s) = \epsilon_\infty + \frac{\omega_{\rm p}^2}{s(s + \nu)} \tag{36}$$

and

$$\epsilon(t) = \epsilon_\infty \delta(t) + \frac{\omega_{\rm p}^2}{\nu}(1 - {\rm e}^{-\nu t}) H(t), \tag{37}$$

where $\epsilon_\infty > 0$ is the optical response, $\omega_{\rm p} > 0$ the plasma frequency and $\nu > 0$ the collision frequency. In this case

it is straightforward to derive the following generalized step response by using standard Laplace transform methods yielding:

$$\begin{aligned}&\epsilon(t) * (1 - \mathrm{e}^{-t/\tau})H(t)\\ &\quad = \epsilon_\infty(1 - \mathrm{e}^{-t/\tau})H(t)\\ &\qquad + \frac{\omega_\mathrm{p}^2}{\nu^2}\left(\frac{\tau^2\nu^2\mathrm{e}^{-t/\tau} - \mathrm{e}^{-\nu t}}{\tau\nu - 1} + \nu t - \tau\nu - 1\right)H(t),\end{aligned} \quad (38)$$

where $\tau > 0$ is the raise time of the generalized step function. It is assumed here that $\tau \neq 1/\nu$. In case the excitation is an ideal unit step function, we can set $\tau = 0$ and obtain

$$\epsilon(t) * H(t) = \epsilon_\infty H(t) + \frac{\omega_\mathrm{p}^2}{\nu^2}(\mathrm{e}^{-\nu t} + \nu t - 1)H(t). \quad (39)$$

The corresponding PR function and its first-order asymptotics are given by

$$\begin{aligned}p(s) &= s\epsilon_\infty + \frac{\omega_\mathrm{p}^2}{s + \nu}\\ &= \begin{cases}\frac{\omega_\mathrm{p}^2}{\nu} + \left(\epsilon_\infty - \frac{\omega_\mathrm{p}^2}{\nu^2}\right)s + o(s) & \text{as } s \hat{\to} 0\\ \epsilon_\infty s + \omega_\mathrm{p}^2 s^{-1} + o(s^{-1}) & \text{as } s \hat{\to} \infty.\end{cases}\end{aligned} \quad (40)$$

We can see that the requirements given by Eq. (17) are not satisfied here and the bound given by Eq. (21) can not be applied. However, the high-frequency asymptotics (3) is valid and we do have the early-time bounds given by Eq. (6) where

$$\begin{aligned}a_{-1} &= 0,\\ b_1 = \epsilon_\infty \quad b_{-1} &= \omega_\mathrm{p}^2,\end{aligned} \quad (41)$$

and there is no static permittivity.

The corresponding early-time bound (23) is then given by

$$|\epsilon(t) * \delta_t f(t) - \epsilon_\infty \delta_t f(t)| \leqslant \omega_\mathrm{p}^2 \delta_t^{-1} f(t). \quad (42)$$

Thus, in the case when the raise time $\tau > 0$, we can write the bound explicitly as

$$\begin{aligned}&|\epsilon(t) * (1 - \mathrm{e}^{-t/\tau})H(t) - \epsilon_\infty(1 - \mathrm{e}^{-t/\tau})H(t)|\\ &\quad \leqslant \omega_\mathrm{p}^2\left(\tau^2(1 - \mathrm{e}^{-t/\tau}) + \tfrac{1}{2}t^2 - \tau t\right)H(t),\end{aligned} \quad (43)$$

and where $\delta_t f(t)$ and $\delta_t^{-1} f(t)$ have been inserted according to Eq. (10). In case the input is the standard unit step function with raise time $\tau = 0$, we have instead $\delta_t f(t) = H(t)$ for which $\delta_t^{-1} f(t) = \frac{1}{2}t^2 H(t)$. The bound in Eq. (43) can now be compared with the corresponding Drude responses in Eqs. (38) and (39). In addition, from Eqs. (27) and (29) we can also infer that the static conductivity ς and the time of no conduction t_nc for the Drude model are given by

$$\varsigma = \frac{\epsilon_0\omega_\mathrm{p}^2}{\nu}, \quad (44)$$

and

$$t_\mathrm{nc} = \frac{1}{\nu}, \quad (45)$$

respectively.

In Fig. 2 is shown the early-time bounds for the generalized step response (43) with asymptotics given by (40) and a comparison with the actual response of the Drude model (38) for gold (Au) according to the free electron model of Olmon *et al.* [30]. Here, $\epsilon_\infty = 1$, $\omega_\mathrm{p} = 1.29 \cdot 10^{16}\,\mathrm{s}^{-1}$ ($\hbar\omega_\mathrm{p} = 8.5\,\mathrm{eV}$) and $\nu = 7.14 \cdot 10^{13}\,\mathrm{s}^{-1}$ ($\hbar\nu = 0.047\,\mathrm{eV}$). The static conductivity according to this model is $\varsigma = 2.1 \cdot 10^7\,\mathrm{S/m}$ and the characteristic time of no conduction is $t_\mathrm{nc} = 14\,\mathrm{fs}$. The plot is made for $t \in [0, 2t_\mathrm{nc}]$ and with $\tau \in \{0, 0.1t_\mathrm{nc}, 0.2t_\mathrm{nc}\}$. Notably, the characteristic frequency $1/t_\mathrm{nc} = 71\,\mathrm{THz}$ is in the intermediate infrared region.

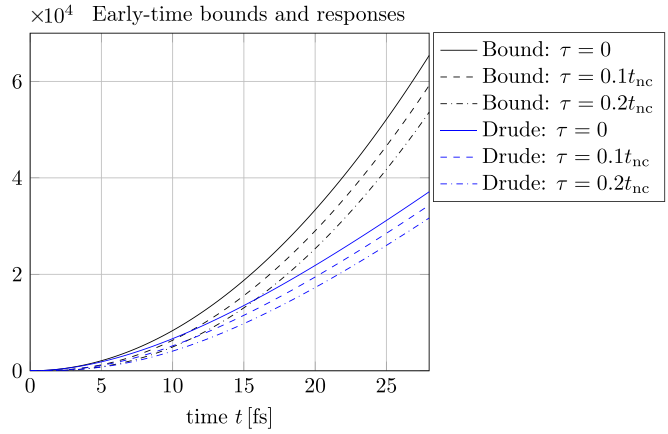

FIG. 2. Early-time bounds for the generalized step response with pulse raise time τ and a comparison with the actual response of the Drude model for gold (Au) according to the free electron model of Olmon *et al.* [30]. The bounds are in black color and the Drude responses are in blue color. The characteristic time of no conduction $t_\mathrm{nc} = 14\,\mathrm{fs}$ is centered in the middle of the plotted time interval.

As we can see in this plot, the quadratic upper bound starts to deviate significantly from the actual step response for $t > t_\mathrm{nc} = 14\,\mathrm{fs}$, which is the time when the material starts behaving adequately as a conductor. This can be observed as the slope (derivative) of the step response (28) becomes a constant ς/ϵ_0 as defined in Eq. (27).

IV. THE BRENDEL-BORMANN MODEL

A. General properties

A widely accepted nonrational model for the dielectric response of metals and amorphous solids is given by the BB model [20,21]. Here, the electric susceptibility function of a single resonance ($j = 1, \ldots, k$) is given by a Gaussian distribution of Lorentzian oscillators as

$$\chi_j(\omega) = \frac{1}{\sqrt{2\pi}\sigma_j}\int_{-\infty}^{\infty} \mathrm{e}^{-(x-\omega_j)^2/2\sigma_j^2}\frac{\omega_{\mathrm{p}j}^2}{x^2 - \omega^2 - \mathrm{i}\omega\nu_j}\mathrm{d}x, \quad (46)$$

where ω_j is the resonance frequency, $\omega_{\mathrm{p}j}$ the plasma frequency of the Lorentzian, ν_j the line width of the Lorentzian and σ_j^2 the variance of the Gaussian distribution. The total dielectric function is then modeled as

$$\epsilon(\omega) = 1 - \frac{\omega_{\mathrm{p}0}^2}{\omega(\omega + \mathrm{i}\nu_0)} + \sum_{j=1}^{k}\chi_j(\omega), \quad (47)$$

where the second term is an ordinary Drude model with parameters $\omega_{\mathrm{p}0}$ and ν_0, cf., Ref. [21, Eq. (11)]. It is noted that there is no static permittivity associated with either of the ordinary Drude model or with the BB model as $\epsilon(\omega)$ is

singular at $\omega = 0$. However, as will become evident below, the static conductivity of the BB model is the same as of the Drude term, i.e., $\varsigma = \epsilon_0\omega_{\mathrm{p}0}^2/\nu_0$, cf., Eq. (44).

The models in Eqs. (46) and (47) are given here in terms of the Fourier-Laplace transform where the Laplace variable is $s = -\mathrm{i}\omega$. Thus, the adequate Herglotz function here is $h(\omega) = \omega\epsilon(\omega)$ and the corresponding PR function is $p(s) = -\mathrm{i}h(\omega) = s\epsilon(s)$, cf., Refs. [4,32]. In Appendix C below is shown that the model (47) is indeed representing a passive material where $\omega\epsilon(\omega)$ is a symmetric Herglotz function.

Let us now investigate the asymptotic properties of the Herglotz function $h(\omega) = \omega\epsilon(\omega)$ given by Eq. (47). For this purpose we may now exploit the fact that $\chi_j(\omega)$ can be expressed as

$$\chi_j(\omega) = \frac{\omega_{\mathrm{p}j}^2\sqrt{\pi}}{2\sqrt{2}\sigma_j\alpha_j}\mathrm{i}\left(w\left(\frac{\alpha_j-\omega_j}{\sqrt{2}\sigma_j}\right)+w\left(\frac{\alpha_j+\omega_j}{\sqrt{2}\sigma_j}\right)\right), \tag{48}$$

where $w(\cdot)$ is the Faddeeva function and $\alpha_j = \sqrt{\omega^2+\mathrm{i}\omega\nu_j}$ where $\mathrm{Im}\{\alpha_j\} > 0$ for $\omega \neq 0$, cf., Refs. [20,21]. In fact, a representation of the BB model based on Eq. (48) is tractable for numerical reasons as well as for analytical purposes. There is a vast literature on the development of fast and accurate numerical methods for the computation of the Faddeeva function, see, *e.g.*, Refs. [33–40], only to mention a few, and a typical application is within quantitative spectroscopy, see *e.g.*, Ref. [41] with references. The analytical properties of the Faddeeva function are furthermore well established and readily applicable as will be demonstrated below. In particular, the Faddeeva function is an entire function defined by $w(z) = \mathrm{e}^{-z^2}\mathrm{erfc}(-\mathrm{i}z)$ where $\mathrm{erfc}(z)$ is the complementary error function $\mathrm{erfc}(z) = \frac{2}{\sqrt{\pi}}\int_z^\infty \mathrm{e}^{-t^2}\mathrm{d}t$ cf., Ref. [42, Eqs. (7.2.1)–(7.2.3)]. From this definition it can readily be shown that $w(-z^*) = w^*(z)$ for all $z \in \mathbb{C}$, cf., *e.g.*, Ref. [43, Eq. (7.1.12)]. The Faddeeva function also has an integral representation given by

$$w(z) = \frac{\mathrm{i}}{\pi}\int_{-\infty}^{\infty}\frac{\mathrm{e}^{-\xi^2}}{z-\xi}\mathrm{d}\xi, \tag{49}$$

which is valid for $\mathrm{Im}\{z\} > 0$ and which is showing that $\mathrm{i}w(z)$ is a Herglotz function and $\mathrm{Re}\{w(z)\} > 0$ for $\mathrm{Im}\{z\} > 0$, cf., [43, Eq. (7.1.4)]. The values of $w(z)$ at the real axis can be inferred by taking the following limit of the integral representation Eq. (49):

$$w(x) = \lim_{y\to 0+} w(x+\mathrm{i}y) = \mathrm{e}^{-x^2} + \frac{\mathrm{i}}{\pi}\fint_{-\infty}^{\infty}\frac{\mathrm{e}^{-\xi^2}}{x-\xi}\mathrm{d}\xi, \tag{50}$$

where $x \in \mathbb{R}$ and the integral is taken in the sense of a Cauchy principal value. The small- and large argument asymptotics of $w(z)$ are furthermore given by

$$w(z) = \begin{cases} 1+\mathrm{i}\frac{2}{\sqrt{\pi}}z+\mathcal{O}\{z^2\}, & \text{as } z\to 0,\\ \mathrm{i}\frac{1}{\sqrt{\pi}}\frac{1}{z}+\mathcal{O}\{\frac{1}{z^3}\}, & \text{as } z\to\infty,\end{cases} \tag{51}$$

where the first expression is a Taylor series expansion at $z = 0$ and the second expansion is valid for $-\pi/4 < \arg(z) < 5\pi/4$, cf., Ref. [42, Eq. (7.6.3)] and Ref. [42, Eq. (7.12.1)], respectively. We will furthermore need the following asymptotic approximation of the function $\alpha_j(\omega)$:

$$\alpha_j(\omega) = \sqrt{\omega^2+\mathrm{i}\omega\nu_j} = \begin{cases}\sqrt{\mathrm{i}\omega\nu_j}+o(\sqrt{\mathrm{i}\omega}) & \text{as } \omega\to 0,\\ \omega+o(\omega), & \text{as } \omega\to\infty,\end{cases} \tag{52}$$

and where the square root must be chosen such that $\mathrm{Im}\{\sqrt{z}\} \geqslant 0$.

By carefully investigating the model (48) in view of the analytical properties given above, it can readily be found that

$$\chi_j(\omega) = \begin{cases}\frac{\mathrm{i}C_j}{\sqrt{\mathrm{i}\omega}}+o\left(\frac{1}{\sqrt{\mathrm{i}\omega}}\right), & \text{as } \omega\to 0,\\ -\frac{\omega_{\mathrm{p}j}^2}{\omega^2}+o\left(\frac{1}{\omega^2}\right), & \text{as } \omega\to\infty,\end{cases} \tag{53}$$

where

$$C_j = \frac{\omega_{\mathrm{p}j}^2}{\sigma_j}\sqrt{\frac{\pi}{2\nu_j}}\mathrm{e}^{-\omega_j^2/2\sigma_j^2}. \tag{54}$$

Thus, the corresponding Herglotz function has the asymptotics

$$\omega\chi_j(\omega) = \begin{cases} o(\omega^{-1}), & \text{as } \omega\to 0,\\ -\omega_{\mathrm{p}j}^2\omega^{-1}+o(\omega^{-1}), & \text{as } \omega\to\infty.\end{cases} \tag{55}$$

In fact, at low frequencies we can see that $\omega\chi_j(\omega) = C_j\sqrt{\mathrm{i}\omega}+o(\sqrt{\mathrm{i}\omega}) = o(\omega^{-1})$, indicating that the only useful information that we can retrieve from the low-frequency asymptotics with regard to our sum rules is that the coefficient $a_{-1} = 0$. For comparison, it is seen that the Drude term is $\omega\chi_0(\omega) = \mathrm{i}\omega_{\mathrm{p}0}^2/\nu_0 + o(1) = o(\omega^{-1})$ for small ω, also of *odd* asymptotic order -1. Hence, similar to the Drude model, our focus here must be on the high-frequency asymptotics (3) together with the associated early-time bounds.

From the analysis above follows that the asymptotics of the positive real function $p(s) = s\epsilon(s)$ corresponding to the BB model given by Eq. (47) is given by

$$p(s) = \begin{cases} o(s^{-1}), & \text{as } s\to 0,\\ s+\sum_{j=0}^k\omega_{\mathrm{p}j}^2 s^{-1}+o(s^{-1}), & \text{as } s\to\infty,\end{cases} \tag{56}$$

and where we have used again that $p(s) = -\mathrm{i}h(\omega)$ and $s = -\mathrm{i}\omega$. We can now conclude that the early-time bounds (22) and (23) as well as Eq. (25) are applicable with $a_{-1} = 0$, $b_1 = \epsilon_\infty = 1$ and $b_{-1} = \omega_{\mathrm{p}}^2$ is the equivalent plasma frequency given by

$$\omega_{\mathrm{p}}^2 = \sum_{j=0}^k\omega_{\mathrm{p}j}^2. \tag{57}$$

To be more specific, let us now introduce the notation $\epsilon = 1+\chi$ where $\chi = \chi_0+\chi_{\mathrm{r}}$ and where χ_0 corresponds to the Drude term and $\chi_{\mathrm{r}} = \sum_{j=1}^k\chi_j$ is the resonant term defined in Eqs. (46) and (47). In Appendix C is shown that the inverse Fourier integral $\chi_{\mathrm{r}}(t)$ as given by (C4) is well defined and real valued due to the symmetry $\chi_{\mathrm{r}}(-\omega) = \chi_{\mathrm{r}}^*(\omega)$ for $\omega \neq 0$, cf., Eq. (C3). From the initial and final value theorems of the Laplace transform together with the asymptotics established

in Eq. (53) follows furthermore that

$$\lim_{t\to 0+}\chi_{\rm r}(t)=\lim_{s\to\infty}s\chi_{\rm r}(s)=0,$$
$$\lim_{t\to +\infty}\chi_{\rm r}(t)=\lim_{s\to 0}s\chi_{\rm r}(s)=0, \tag{58}$$

and where we have employed again that $s=-{\rm i}\omega$. In particular, we can see that the resonant term $\chi_{\rm r}$ does not contribute to the static conductivity. Thus, from Eq. (27) we can now infer that the static conductivity for the BB model is the same as for the corresponding Drude term

$$\varsigma=\frac{\epsilon_0\omega_{\rm p0}^2}{\nu_0}, \tag{59}$$

but the time of no conduction (29) becomes

$$t_{\rm nc}=\frac{\omega_{\rm p0}^2}{\omega_{\rm p}^2\nu_0}<\frac{1}{\nu_0}. \tag{60}$$

We can conclude that the early-time bounds for the step response, Eqs. (22) and (23), with the BB model are very similar to the corresponding bounds for the Drude term χ_0, only with a larger plasma frequency $\omega_{\rm p}>\omega_{\rm p0}$ indicating a faster response at (very) early times. At late times the response is governed by the Drude term χ_0 and its associated static conductivity ς, as dictated by Eqs. (27) and (28), cf., also the Drude example shown in Fig. 2.

The optical constants of 11 metals have been modeled with BB parameters $(\omega_{{\rm p}j},\sigma_j,\omega_j,\nu_j)$ and fitted to experimental data in Ref. [21, Eq. (11) with parameters from Table I and Table III]. The corresponding plasma frequency $\omega_{\rm p}$, the static conductivity ς and the characteristic time $t_{\rm nc}$ are calculated here according to Eqs. (57), (59), and (60) and summarized in Table I below.

As will be demonstrated in the numerical example based on the BB parameters for gold (Au) below, the contribution to the early time response from the resonant term $\chi_{\rm r}(t)$ is very minor (very early) and the time of no conduction is essentially governed by the Drude term with $t_{\rm nc}=1/\nu_0$.

B. Numerical evaluation of the impulse response

To the authors knowledge, an explicit analytical expression for the impulse or step responses of the resonant part of the BB model is nontrivial to derive and does not exist in a simple manner as for the Drude model treated above. We will therefore consider here a numerical evaluation of the impulse response by using the FFT. This is possible to achieve for the impulse response $\chi_{\rm r}(t)$ but not for the step response $\chi_{\rm r}(t)*H(t)$. The fundamental reason for this is very simple: A well behaved (converging) approximation of the inverse Fourier transform (C4) by using the FFT is based on truncated sampling in the time domain as well as in the frequency domain and the corresponding Nyquist-Shannon sampling theorems must therefore be satisfied asymptotically as the size of the FFT increases. The function under consideration must therefore be asymptotically band limited in frequency as well as in time to avoid aliasing in either domain. This is indeed the case for the resonant term $\chi_{\rm r}(t)$ as we can see from the asymptotic properties expressed in Eqs. (53) and (58). However, this is not the case for the step response $\chi_{\rm r}(t)*H(t)$ whose Laplace transform $\chi_{\rm r}(s)/s$ is clearly not integrable at the real ω axis. To this end, it should be observed that the square root singularity of $\chi_{\rm r}(s)$ at $s=0$ is weak in the sense of Ref. [44, Eq. (2.4)] and the integral in Eq. (C4) is absolutely convergent, whereas the singularity of $\chi_{\rm r}(s)/s$ is strong (not weak). Hence, $\chi_{\rm r}(t)*H(t)$ does not have a final value. But of course, once $\chi_{\rm r}(t)$ has been obtained numerically, its step response could easily be approximated by discrete-time convolution with $H(t)$, etc.

Let us now turn to the numerical computation of the susceptibility function $\chi(t)=\chi_0(t)+\chi_{\rm r}(t)$ and where the Drude term is obtained directly from Eq. (37) as

$$\chi_0(t)=\frac{\omega_{\rm p0}^2}{\nu_0}(1-{\rm e}^{-\nu_0 t})H(t). \tag{61}$$

The resonant term is now obtained by approximating the integral in Eq. (C4) by performing the following FFT:

$$\chi_{\rm r}(t_n)=\sum_{k=0}^{N-1}\chi_{\rm r}(f_k){\rm e}^{-{\rm i}\frac{2\pi}{N}kn}\Delta f,\quad n=0,1,\ldots,N-1, \tag{62}$$

where N is the size of the FFT (preferable a power of 2), $t_n=n\Delta t$ the time samples, Δt the sampling time, $f_{\rm s}=1/\Delta t$ the sampling rate and $f_k=k\Delta f$ the frequency samples where $\Delta f=f_{\rm s}/N$. Clearly, with $t=n\Delta t$ and $\omega=2\pi f_k$, we have

$$\omega t=2\pi k\frac{f_{\rm s}}{N}n\Delta t=\frac{2\pi}{N}kn. \tag{63}$$

As always with the FFT, the TD sequences $\chi_{\rm r}(t_n)$ as well as the frequency domain sequences $\chi_{\rm r}(f_k)$ must be considered to be periodic with period N. Hence, in order to account for the symmetry $\chi_{\rm r}(-\omega)=\chi_{\rm r}^*(\omega)$ we take samples $\chi_{\rm r}(f_k)$ in accordance with the continuous model (48) for $k=1,\ldots,N/2-1$, and then choose

$$\chi_{\rm r}(f_k)=\chi_{\rm r}^*(f_{N-k}), \tag{64}$$

for $k=N/2+1,\ldots,N-1$. Without loss of significant numerical accuracy we can also choose $\chi_{\rm r}(f_0)=\chi_{\rm r}(f_{N/2})=0$.

TABLE I. Plasma frequencies $\omega_{\rm p}$ and $\omega_{\rm p0}$, static conductivity ς, Drude parameter $1/\nu_0$ and the characteristic time of no conduction $t_{\rm nc}$ for 11 metals retrieved from the BB models given by Ref. [21, Tables I and III].

$\omega_{\rm p}\backslash$ Xy	Ag	Au	Cu	Al	Be	Cr	Ni	Pd	Pt	Ti	W
$\hbar\omega_{\rm p}$ [eV]	21.2	17.0	14.4	14.9	17.3	13.9	17.9	13.4	19.1	8.3	22.9
$\hbar\omega_{\rm p0}$ [eV]	8.2	7.9	8.1	10.9	5.3	4.2	4.6	5.6	5.5	2.6	5.9
ς [10^7S/m]	1.8	1.7	3.0	3.4	1.1	0.50	1.3	4.7	0.52	0.13	0.81
$1/\nu_0$ [fs]	13.4	13.2	21.9	14.0	18.8	13.7	29.9	73.1	8.23	9.82	11.6
$t_{\rm nc}$ [fs]	2.00	2.85	6.97	7.40	1.75	1.26	1.97	12.6	0.69	0.96	0.76

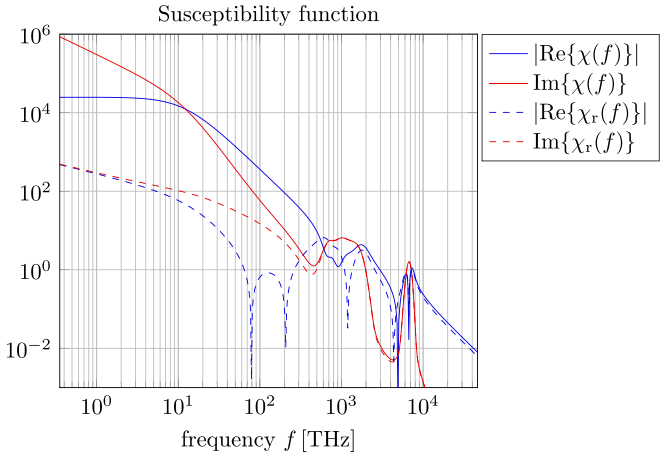

FIG. 3. Real and imaginary parts of the Brendel-Bormann (BB) model in the frequency domain $\chi(f) = \chi_0(f) + \chi_\mathrm{r}(f)$ (solid lines) in comparison to its resonant part $\chi_\mathrm{r}(f)$ (dashed lines). The real parts are plotted here in blue color and the imaginary parts in red color. The plot is in logarithmic scale and covers half of the computational domain of the FFT, i.e., $f \in [1/N, 1/2]f_\mathrm{s}$ and where $N = 2^{18}$ and $f_\mathrm{s}/2 = 46341$ THz.

The total time period is $T = N\Delta t$ and the total frequency period is $f_\mathrm{s} = N\Delta f$. To obtain a numerically converging procedure as N is growing we can now proceed as follows. We start by choosing a suitable FFT size N_0 and a suitable sampling rate $f_{\mathrm{s}0} = 1/\Delta t_0$. The corresponding time period is $T_0 = N_0\Delta t_0$ and the frequency resolution is $\Delta f_0 = f_{\mathrm{s}0}/N_0$. We can then evaluate the result and choose another value $N > N_0$ (preferable another power of 2) and let

$$f_\mathrm{s} = f_{\mathrm{s}0}\sqrt{\frac{N}{N_0}}, \tag{65}$$

which is directly yielding

$$T = T_0\sqrt{\frac{N}{N_0}}, \quad \Delta t = \Delta t_0\sqrt{\frac{N_0}{N}}, \quad \Delta f = \Delta f_0\sqrt{\frac{N_0}{N}}. \tag{66}$$

Hence, as N is growing also f_s and T are growing at the same time as Δt and Δf are getting smaller and the bandwidth-time product is $f_\mathrm{s}T = f_{\mathrm{s}0}T_0N/N_0$. Notably, the exclusion of the frequency point $f_0 = 0$ in Eq. (62) by setting $\chi_\mathrm{r}(f_0) = 0$ does not pose a problem here as the square root singularity at $\omega = 0$ is only weak (integrable) and $\Delta f \to 0$ as $N \to \infty$.

In Figs. 3 through 6 are shown the results of a computation of bounds and responses associated with the BB model for gold (Au) with parameters from [21, Tables I and Table III]. The Drude term is given analytically by Eq. (61) and the resonant term is obtained numerically by using the FFT as in Eq. (62) with parameters summarized in Tables I and II. Here, we choose initially $N_0 = 2^{15}$, $\Delta f_0 = 1$ THz and hence $f_{\mathrm{s}0} = N_0\Delta f_0 = 2^{15}$ THz. A very good convergence was obtained already at this time-frequency resolution and there was no reason to go beyond $N = 2^{18}$ which was used to generate the plots with $\Delta f = 0.35$ THz and $\Delta t = 0.01$ fs. The Faddeeva function was evaluated numerically by using the Abrarov-implementation [39] which is optimized for accuracy rather than speed. The typical computation time on a standard laptop computer (MacBook Pro with 2.6 GHz 6-Core Intel Core i7 processor (2019)) was 0.1 s for computing the frequency response $\chi_\mathrm{r}(\omega)$ and 0.005 s for computing the FFT yielding the final time response $\chi_\mathrm{r}(t)$.

TABLE II. Parameters of the resonant term χ_r according to the Brendel-Bormann model for gold (Au) given by Ref. [21, Tables I and III].

$j\backslash X_j$ [THz]	$\omega_{\mathrm{p}j}$	σ_j	ω_j	ν_j
$j = 1$	507	179	53	18
$j = 2$	488	84	698	8.5
$j = 3$	1220	201	984	20
$j = 4$	1851	301	1484	30
$j = 5$	2803	434	6763	43

As we can see from the frequency responses plotted in Fig. 3, the resonant term $\chi_\mathrm{r}(f)$ is quite negligible in comparison to the Drude term at frequencies lower than 100 THz. Thus, the Drude response is dominating at late times which is clearly seen in Fig. 5. At higher frequencies however, the resonant term will start to dominate, and in particular close to its highest resonance at 6763 THz which is emphasized in Fig. 4. This is also clearly visible as the short time ringing effect illustrated in Fig. 6. Note also that the high frequency asymptotes of the BB model $\chi(\omega) \sim -\omega_\mathrm{p}^2\omega^{-2}$ and its Drude term $\chi_0(\omega) \sim -\omega_{\mathrm{p}0}^2\omega^{-2}$, are manifested in the TD as the short time asymptotes (and upper bounds), $\chi(t) \sim \omega_\mathrm{p}^2 t$ and $\chi_0(t) \sim \omega_{\mathrm{p}0}^2 t$, respectively, and where $\omega_\mathrm{p}^2 > \omega_{\mathrm{p}0}^2$, cf., Figs. 5 and 6.

It should finally be mentioned that the parameters of the BB model employed here have not been optimized for early times, but rather for some specific frequency ranges as reported in Ref. [21, Fig. 2], i.e., 48–1209 THz for gold (Au). It is therefore not at all clear if the modeled BB resonance at 6763 THz (wavelength 44 nm) has a physical significance in the TD, and it is included here merely to demonstrate the general theory for deriving physical bounds and to give examples

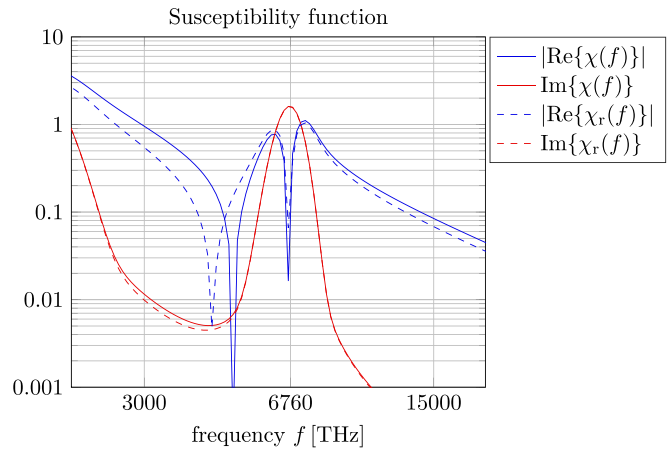

FIG. 4. Same plot as in Fig. 3, only over the more narrow frequency interval centered around the highest resonance of $\chi_\mathrm{r}(f)$ at 6763 THz. Here, the two plots are almost coincident indicating that the resonant term $\chi_\mathrm{r}(f)$ is dominating over the Drude term $\chi_0(f)$.

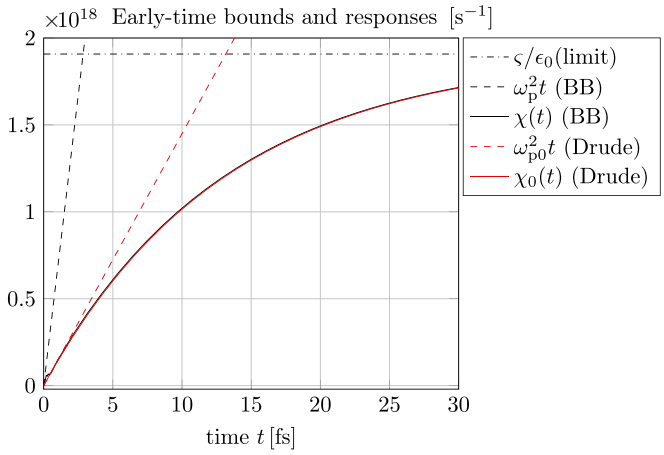

FIG. 5. Early-time time bounds (dashed lines) and impulse responses (solid lines) for the Brendel-Bormann (BB) model in the time domain $\chi(t) = \chi_0(t) + \chi_r(t)$ in comparison to its Drude term $\chi_0(t)$. The BB model is plotted here in black and the Drude term in red. The horizontal dashed-dotted line indicates the final value ς/ϵ_0 where ς is the static conductivity. On this time scale the BB and the Drude responses are almost coincident and the (corner) time of no conduction for the dominating Drude term is $t_{nc} = 1/\nu_0 = 13.2\,\text{fs}$.

of responses associated with a particular model. To this end, the time- and frequency domain analyses together provide a very useful tool to make the correct physical interpretation of the model at hand. In particular, for high-speed electronic or optoelectronic applications with switching frequencies in the intermediate infrared range less than 100 THz, we can see that the adequate time scales are in the order of 10 fs or more. From the results above, it should then be quite clear that it is the Drude mechanism of the BB model that governs the early time responses and the corresponding time of no conduction $t_{nc} = 1/\nu_0$ is the most relevant parameter in this context. The BB resonance at 6763 THz should furthermore be regarded as part of the optical response of the material, here modeled by $\epsilon_\infty\delta(t)$. For the purpose of analyzing short time responses of thin metallic films or other optical interference

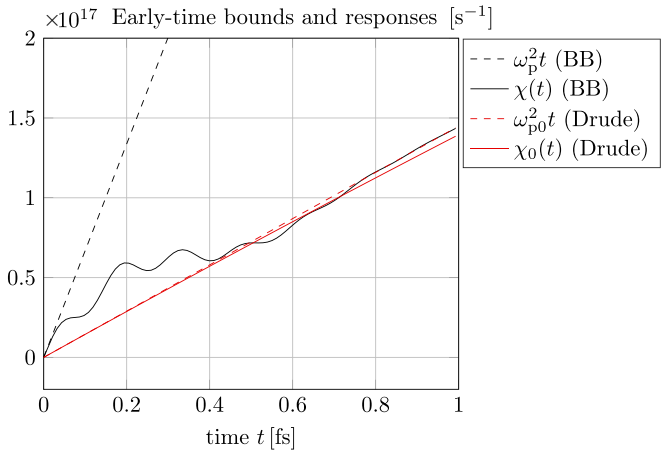

FIG. 6. Same plot as in Fig. 5, only on a much shorter time scale. The short time ringing effect is due to the highest resonance of $\chi_r(t)$ at 6763 THz corresponding to a period of 0.15 fs, cf., also Fig. 4.

devices in connection with the BB model, it may therefore be suitable to adapt its parameters to larger frequency ranges, preferably to exclude high-frequency resonances outside the modeled domain, and to include high quality *a priori* values (measurements) of the static conductivity ς in accordance with the asymptotics given by Eq. (59).

V. SUMMARY AND CONCLUSIONS

Physical limitations on the time-domain (TD) response of a passive system has been presented in this paper. As a canonical example we have focused on the physical meaning and modeling of the optical response of a passive material. For this purpose, we have also revisited and re-established the well known and highly appreciated, but also sometimes misunderstood, Brendel-Borman (BB) oscillator model as a perfectly sound physical model for the permittivity of a passive material. The theory is based on Cauer's representation of an arbitrary positive real (PR) function together with associated sum rules and exploits the unilateral Laplace transform to derive rigorous bounds directly in the TD. The advantage of this approach is the ease by which rigorous physical bounds can be derived by exploiting the integral representation, its positive generating measure, and associated sum rules. The method is, however, limited to PR functions having some odd ordered low- and/or high-frequency asymptotic expansion for which the required sum rule exists. Hence, this field will be open to explore other subclasses of linear, time-invariant and casual systems beyond passive systems, as suggested in Refs. [9,10].

APPENDIX A: POSITIVE REAL FUNCTIONS

1. Basic properties

The set of PR functions $\{p(s)\}$ is equivalent to the set of symmetric Herglotz functions $\{h(z)\}$ via the transformation $p(s) = -ih(is)$ where $s = -iz$. Their basic properties can therefore be deduced from one another based on an extensive literature found in, *e.g.*, Refs. [1,2,4–7] with references, and where we will employ here in particular the survey given in Ref. [4]. For convenience, it is practical here to set $z = x + iy$ and $s = \sigma - i\omega$ so that $\omega = x$ (frequency) and $\sigma = y$ (damping, or loss factor). The more conventional definition for the Laplace variable $s = \sigma + j\omega$ is then obtained simply by making the substitution $i = -j$.

A PR function is a holomorphic function defined on the open right half-plane $\mathbb{C}_+ = \{s \in \mathbb{C} | \text{Re}\{s\} > 0\}$ where its real part is non-negative, i.e., $\text{Re}\{p(s)\} \geqslant 0$ for $s \in \mathbb{C}_+$ and which satisfies the following symmetry:

$$p(s) = p^*(s^*), \tag{A1}$$

cf., *e.g.*, [4, Definition 20.3] and [2, Chap. 10.4]. Consequently, the corresponding symmetric Herglotz function $h(z) = ip(-iz)$ is a holomorphic function defined on the open upper half-plane $\mathbb{C}^+ = \{z \in \mathbb{C} | \text{Im}\{z\} > 0\}$ where its imaginary part is non-negative, i.e., $\text{Im}\{h(z)\} \geqslant 0$ for $z \in \mathbb{C}^+$. Symmetric Herglotz functions satisfy the symmetry requirement

$$h(z) = -h^*(-z^*). \tag{A2}$$

Any PR function is uniquely given by Cauer's representation Ref. [2, Chap. 10.5]

$$p(s) = bs + \int_{-\infty}^{\infty} \frac{s}{s^2+\xi^2} \mathrm{d}\beta(\xi), \tag{A3}$$

where $b \geqslant 0$ and the positive Borel measure $\beta(\xi)$ is the same as for the corresponding Herglotz function Ref. [4, Eq. (20.13)] with growth condition

$$\int_{-\infty}^{\infty} \frac{\mathrm{d}\beta(\xi)}{1+\xi^2} < \infty. \tag{A4}$$

The constant b is determined by

$$b = \lim_{s \hat{\to} \infty} \frac{p(s)}{s}, \tag{A5}$$

where the nontangential limit is taken in the right half-plane ($|s| \to \infty$ in the Stoltz cone $\varphi - \pi/2 \leqslant \arg s \leqslant \pi/2 - \varphi$ for any $\varphi \in (0, \pi/2]$). The positive measure β is furthermore uniquely determined by the PR function [Herglotz function $h(z) = \mathrm{i}p(s)$] from the Stieltjes inversion formula, see [5,7]. In particular, in the case when the measure is absolutely continuous we may write $\mathrm{d}\beta(\xi) = \beta'(\xi)\mathrm{d}\xi$ where $\beta'(\xi)$ is the density of the measure and where

$$\beta'(\xi) = \frac{1}{\pi} \lim_{\sigma \to 0+} \mathrm{Re}\{p(\sigma - \mathrm{i}\xi)\}. \tag{A6}$$

It is noted that the measure is even and we have that $\mathrm{d}\beta(-\xi) = -\mathrm{d}\beta(\xi)$ and thus $\beta'(-\xi) = \beta'(\xi)$. For point masses we have $\beta(\{\xi_0\}) = \beta(\{-\xi_0\})$.

It is readily seen (by using residue calculus) that a real constant $p(s) = C$ with $C > 0$ can be generated by the constant measure $\mathrm{d}\beta(t) = \frac{1}{\pi} C \mathrm{d}t$. It follows directly from the symmetry requirement (A1) [as well as from the representation (A3)] that $p(s)$ is real valued for real valued s. It can furthermore be shown that $\mathrm{Re}\{p(s)\} > 0$ for $s \in \mathbb{C}_+$ unless $p(s) \equiv 0$. Thus, it is perfectly safe (except for the trivial case $p(s) \equiv 0$) to generate new PR functions by inversion $1/p(s)$ as well as by composition $p_1(p_2(s))$ where both p_1 and p_2 are PR functions.

It can be shown that the measure β has a point mass at the point $\xi_0 \in \mathbb{R}$ if and only if the limit

$$\beta(\{\xi_0\}) = \lim_{s \hat{\to} \mathrm{i}\xi_0} (s - \mathrm{i}\xi_0) p(s) > 0. \tag{A7}$$

A simple example is $\mathrm{d}\beta(\xi) = c\delta(\xi)\mathrm{d}\xi$ generating the PR function $p(s) = \frac{c}{s}$ where $c = \beta(\{0\}) > 0$ and $\delta(\xi)$ is the Dirac delta function.

For an asymptotic expansion of the form $p(s) \sim \sum_n c_n s^n + o(\cdot)$ (either for $s \hat{\to} 0$ or $s \hat{\to} \infty$) it is readily seen that the symmetry (A1) implies that all coefficients c_n must be real valued. The relationship between the corresponding coefficients for a symmetric Herglotz function with $h(z) \sim \sum_n \tilde{c}_n z^n + o(\cdot)$, is thus given by $c_n = -\mathrm{i}^{n+1}\tilde{c}_n$. Hence, with n even we have $\tilde{c}_{n-1} = -(-1)^{n/2} c_{n-1}$ for odd order coefficients, etc.

2. Sum rules for positive real functions

Based on Ref. [4, Theorem 20.2 and 20.3] we can now formulate the following definitions and the corresponding sum rules for PR functions. A PR function p is said to admit at $s = 0$ an *odd* asymptotic expansion of odd order M if for $M \geqslant -1$ there exist real numbers $a_{-1}, a_1, \ldots, a_M$ such that p can be written

$$p(s) = a_{-1}s^{-1} + a_1 s + \cdots + a_M s^M + o(s^M), \quad \text{as } s \hat{\to} 0. \tag{A8}$$

Similarly, a PR function p is said to admit at $s = \infty$ an *odd* asymptotic expansion of odd order M if for $M \geqslant -1$ there exist real numbers $b_1, b_{-1}, \ldots, b_{-M}$ such that p can be written

$$p(s) = b_1 s + b_{-1}s^{-1} + \cdots + b_{-M}s^{-M} + o(s^{-M}), \quad \text{as } s \hat{\to} \infty. \tag{A9}$$

It can be shown that every PR function has an odd asymptotic expansion both at $s = 0$ and at $s = \infty$ of order -1, and we have $a_{-1} = \lim_{s \hat{\to} 0} sp(s) = \beta(\{0\}) \geqslant 0$ and $b_1 = \lim_{s \hat{\to} \infty} s^{-1}p(s) \geqslant 0$.

For a positive real function to admit at $s = 0$ an *odd* asymptotic expansion of odd order M where $M \geqslant 1$, it is both necessary and sufficient that the following sum rules (moments of the measure) hold:

$$\int_{\mathbb{R}\setminus\{0\}} \frac{\mathrm{d}\beta(\xi)}{\xi^n} = \begin{cases} a_1 - b_1 & n = 2 \\ -(-1)^{n/2} a_{n-1} & n = 4, 6, \ldots, M+1. \end{cases} \tag{A10}$$

As a consequence, we see also that $a_1 \geqslant b_1$. Similarly, for a positive real function to admit at $s = \infty$ an *odd* asymptotic expansion of odd order M where $M \geqslant 1$, it is both necessary and sufficient that the following sum rules (moments of the measure) hold:

$$\int_{\mathbb{R}\setminus\{0\}} \xi^n \mathrm{d}\beta(\xi) = \begin{cases} b_{-1} - a_{-1} & n = 0 \\ (-1)^{n/2} b_{-n-1} & n = 2, 4, \ldots, M-1. \end{cases} \tag{A11}$$

As a consequence, we see also that $b_{-1} \geqslant a_{-1}$. In Eqs. (A10) and (A11) it is also possible to make the following identification:

$$\lim_{\varepsilon \to 0+} \lim_{\sigma \to 0+} \frac{1}{\pi} \int_{\varepsilon < |\xi| < 1/\varepsilon} \xi^{\pm n} \mathrm{Re}\{p(\sigma - \mathrm{i}\xi)\} \mathrm{d}\xi = \int_{\mathbb{R}\setminus\{0\}} \xi^{\pm n} \mathrm{d}\beta(\xi) \tag{A12}$$

as in Eq. (A6), cf., also *e.g.*, Refs. [4, Eq. (20.10)] and [6, Theorem 3.2.1]. It is important to notice here that a possible point mass at $\xi = 0$ is not included in the integrals expressed in Eqs. (A10) and (A11).

It is finally noted that the sum rules expressed in Ref. [4, Theorem 20.2 and 20.3] are given for general Herglotz functions without any assumptions about symmetry. It is also noticed that these theorems require that the corresponding asymptotic expansion coefficients are *real valued* up to the required order. The even ordered coefficients are purely imaginary for a symmetric Herglotz function, and hence follows the requirement of having an odd ordered asymptotic expansion for symmetric Herglotz functions as well as for PR functions up to the required order, as in Eqs. (A8) and (A9).

APPENDIX B: THE THOMAS-REICHE-KUHN SUM RULE AND THE CLASSICAL OPTICAL THEOREM

The sum rules presented in the previous section were defined solely in terms of the specific integral identities (A10) and (A11) for positive real functions. The terminology using sum rules is however naturally borrowed from quantum mechanics. Below we will briefly discuss the close connection between the Thomas-Reiche-Kuhn sum rule for an atomic oscillator and the classical optical theorem for a small dipole scatterer. As an application we will furthermore demonstrate the usefulness of the sum rules to obtain normalized BB line shapes for absorption.

Based on quantum mechanical principles, it can be shown that the absorption cross section of a small atomic (dipole) oscillator can be expressed (in SI units) as

$$\sigma_{\rm abs} = \frac{\pi \eta_0 e^2}{2m} \sum_n f_{ni} \delta(\omega - \omega_{ni}), \tag{B1}$$

where the oscillator strengths f_{ni} are given by

$$f_{ni} = \frac{2m\omega_{ni}}{\hbar} |\langle n|x|i\rangle|^2 \tag{B2}$$

and where $\eta_0 = \sqrt{\mu_0/\epsilon_0}$ is the impedance of vacuum, e the dipole charge, x the position operator, $H_0|n\rangle = \hbar\omega_n|n\rangle$, $\omega_{ni} = \omega_n - \omega_i$ and where $H_0 = p^2/2m$ is the Hamiltonian of the oscillator with mass m and momentum p ($p^2 = p_x^2 + p_y^2 + p_z^2$), cf., Ref. [45, p. 368]. The Thomas-Reiche-Kuhn sum rule is furthermore given by

$$\sum_n f_{ni} = 1, \tag{B3}$$

and which can be shown solely by using quantum mechanical commutator properties for x and p, and in particular the identity $[x, [x, H_0]] = -\hbar^2/m$. It should be observed here that no scattering or line broadening is assumed, only absorption to an excited state $|n\rangle$ where $|i\rangle$ represents the ground state, and hence $\omega_{ni} > 0$. From the above we find the following integral identity (also referred to here as a sum rule)

$$\int_0^\infty \sigma_{\rm abs} {\rm d}\omega = \frac{\pi \eta_0 e^2}{2m}. \tag{B4}$$

Let us now turn to classical physics and the mathematical theory of symmetric Herglotz functions (equivalent to PR functions). The classical optical theorem for a small isotropic electric dipole scatterer can then be expressed is terms of its total (or extinction) cross section as

$$\sigma_{\rm t} = {\rm Im}\{h(\omega)\}, \tag{B5}$$

where the adequate Herglotz function $h(\omega)$ is defined by

$$h(\omega) = \frac{\omega}{{\rm c}_0}\alpha(\omega), \tag{B6}$$

and where ${\rm c}_0$ is the speed of light in vacuum and $\alpha(\omega)$ the polarizability of the scatterer, cf., Ref. [46, pp. 71 and 140] and Ref. [47, pp. 227–230, 272]. For a classical Lorentzian oscillator with mass m, charge e, friction constant $m\nu$ and spring constant $m\omega_0^2$, we obtain

$$h(\omega) = \frac{\omega_{\rm p}^2 \omega}{\omega_0^2 - \omega^2 - {\rm i}\omega\nu}, \tag{B7}$$

and where $\omega_{\rm p}^2 = \frac{\eta_0 e^2}{m}$. In terms of the Herglotz function $h(\omega)$ where $p(s) = -{\rm i}h(\omega)$ and $s = -{\rm i}\omega$, the density of the measure (A6) is

$$\beta'(\omega) = \frac{1}{\pi}{\rm Re}\{p(-{\rm i}\omega)\} = \frac{1}{\pi}{\rm Im}\{h(\omega)\}, \tag{B8}$$

and the sum rule in Eq. (A11) for $n = 0$ becomes

$$\int_0^\infty \sigma_{\rm t} {\rm d}\omega = \int_0^\infty {\rm Im}\{h(\omega)\}{\rm d}\omega = \frac{\pi}{2}\omega_{\rm p}^2 = \frac{\pi \eta_0 e^2}{2m}, \tag{B9}$$

where we have exploited the symmetry of the measure and observed that the asymptotic coefficients are $a_{-1} = 0$ and $b_{-1} = \omega_{\rm p}^2$. Hence, under the assumption that scattering can be ignored this result is the same as in Eq. (B4).

Let us finally apply the sum rule (A11) to the BB model. In particular, as is customary in, *e.g.*, atmospheric spectroscopy [41], we can define normalized line shape functions for the absorption as follows. To this end, we can scale the model (48) appropriately and define the following BB model for the multiresonant polarizability

$$\frac{\alpha(\omega)}{{\rm c}_0} = \sum_{j=1}^k \frac{S_j}{\sqrt{2\pi}\sigma_j} \frac{\rm i}{\alpha_j} \left(w\left(\frac{\alpha_j - \omega_j}{\sqrt{2}\sigma_j}\right) + w\left(\frac{\alpha_j + \omega_j}{\sqrt{2}\sigma_j}\right)\right), \tag{B10}$$

where the line strength parameters have been chosen as $S_j = \pi\omega_{pj}^2/2$. Based on the asymptotics given by Eq. (55) and the relation (B8) together with the sum rule (A11) for $n = 0$, we can now define the (nontrivial) normalized line shape functions

$$l_j(\omega) = \frac{1}{\sqrt{2\pi}\sigma_j} {\rm Im}\left\{ \frac{{\rm i}\omega}{\alpha_j} \left(w\left(\frac{\alpha_j - \omega_j}{\sqrt{2}\sigma_j}\right) + w\left(\frac{\alpha_j + \omega_j}{\sqrt{2}\sigma_j}\right)\right)\right\}, \tag{B11}$$

where $\int l_j(\omega){\rm d}\omega = 1$ and write the optical theorem as

$$\sigma_{\rm t} = {\rm Im}\left\{\frac{\omega}{{\rm c}_0}\alpha(\omega)\right\} = \sum_{j=1}^k S_j l_j(\omega) \tag{B12}$$

so that

$$\int_0^\infty \sigma_{\rm t} {\rm d}\omega = \sum_{j=1}^k S_j. \tag{B13}$$

APPENDIX C: ON THE PHYSICAL REALIZABILITY OF THE BRENDEL-BORMANN MODEL

It has been claimed that the BB model, Eq. (46), is unphysical as it is noncausal and asymmetric [22,23]. Allegedly, the model does not (1) satisfy the Kramers-Kronig relations and (2) correspond to a real valued TD expression (inverse Fourier transform), see in particular Refs. [22, Fig. 1] and [23, Sec. 2 B]. It will be shown here that neither of these claims are true.

It is indeed sufficient to consider the definition made in Eq. (46) to realize that the BB model generates a symmetric Herglotz function since $\omega\chi_j(\omega)$ is in the positive cone generated by the Gaussian distribution of rational functions (Lorentzian oscillators) $\omega\omega_{\mathrm{p}j}^2/(x^2-\omega^2-\mathrm{i}\omega\nu_j)$ which are all symmetric Herglotz functions for any $x\in\mathbb{R}$. Here, the resulting Herglotz function is denoted $h(\omega)=\omega\chi_j(\omega)$ and the corresponding PR function is $p(s)=-\mathrm{i}h(\omega)=s\chi_j(s)$ where $s=-\mathrm{i}\omega$, cf., Refs. [4,32]. Now, since the model given by Eq. (46) implies that $\omega\chi_j(\omega)$ is a symmetric Herglotz function it automatically represents a passive system according to the realizability theorem Ref. [2, Theorem 10.6–1]. Any passive system is also causal Ref. [2, Chap. 10.3] and hence satisfies the required Kramers-Kronig relations, cf., also Ref. [4]. The corresponding time-domain expression is real valued due to the symmetry $p(s^*)=p^*(s)$, or equivalently $h(-\omega^*)=-h^*(\omega)$. The same assertments can be made also about the combined model (47) which is just a positive combination of BB models and a Drude model.

Now, it may be useful to contemplate somewhat further upon the rationale for making the incorrect claims (1) and (2) referred to as above, cf., Refs. [22,23]. Their argument to support (1) is that the singularity of $\chi(\omega)$ at $\omega=0$ implies that the susceptibility function must be noncausal due to Titchmarsh's theorem. If this claim was true then also the Drude model (which is singular at $\omega=0$) would be noncausal. This is clearly a contradiction. It is important to note here that Titchmarsh's theorem Ref. [1, Theorem 1.6.1] prescribes analyticity in an open half plane which does not exclude the possibility to have singularities at the real line. But even more importantly, the Titchmarsh's theorem refers only to functions that are square integrable in the frequency domain. Based on the asymptotics given by Eq. (53) we can see that the function $\chi_{\mathrm{r}}(\omega)$ has a square root singularity at $\omega=0$, and the function is therefore not square integrable. Thus, the Titchmarsh's theorem does not apply here at all. However, the function $\chi_{\mathrm{r}}(\omega)$ is *absolutely integrable* and its inverse Fourier transform therefore exists as a bounded function. It may also be observed here that causality of the BB model follows simply by the classical Jordan's lemma [48, p. 300] since $\chi(s)$ is analytical in the open right half plane and where $\chi(s)\to 0$ as $s\to\infty$.

The second claim (2) is about nonsymmetry (non-Hermiticity) and seems to be based solely on a numerical implementation of the susceptibility function as shown in Ref. [22, Fig. 1], and the authors do indeed remark that the result is somewhat perplexing. The misconception here is most likely due to an incorrect use of the complex valued square root producing a non-negative real part. It may therefore be instructive here to verify the required symmetry based directly on the explicit representation (48) since it is very important for numerical implementations. To simplify this expression we write here

$$\chi(\omega)=\frac{\mathrm{i}D}{\alpha(\omega)}\left(w\left(\frac{\alpha(\omega)-\omega_0}{\sqrt{2}\sigma}\right)+w\left(\frac{\alpha(\omega)+\omega_0}{\sqrt{2}\sigma}\right)\right), \tag{C1}$$

where $\alpha(\omega)=\sqrt{\omega^2+\mathrm{i}\omega\nu}$, $\mathrm{Im}\{\alpha(\omega)\}>0$ and where $D=\omega_{\mathrm{p}}^2\sqrt{\pi}/2\sqrt{2}\sigma$, ω_{p}, ω_0, σ and ν are (positive) constants. Now, the derivation of the expression (C1) or (48) is based on the integral representation (49) and hence requires that $\mathrm{Im}\{\alpha(\omega)\}>0$ for $\omega\neq 0$. This will be achieved by defining the square root with a branch cut along the positive real axis so that $\sqrt{z}=\sqrt{|z|}\mathrm{e}^{\mathrm{i}\theta/2}$ where $z=|z|\mathrm{e}^{\mathrm{i}\theta}$ and $0\leqslant\theta<2\pi$ so that $\mathrm{Im}\{\sqrt{z}\}\geqslant 0$. Notably, this is in contrast to the otherwise very common principal square root where $-\pi<\theta\leqslant\pi$, $\mathrm{Re}\{\sqrt{z}\}\geqslant 0$ and which is implemented in, *e.g.*, ™MATLAB. By taking $z=\omega^2+\mathrm{i}\omega\nu$ as a holomorphic function of ω where $\nu>0$, it is readily seen that $0<\theta<2\pi$ when $\mathrm{Im}\{\omega\}>0$. Indeed, the same range can also be chosen when $\mathrm{Im}\{\omega\}=0$ (ω is real valued) and $\omega\neq 0$. Hence, under these circumstances we can employ our definition of the square root and find that $\mathrm{Im}\{\sqrt{z}\}>0$ as well as the identity $\sqrt{z^*}=-(\sqrt{z})^*$ provided that $0<\theta<2\pi$. These considerations implies now that $\alpha(\omega)$ is a Herglotz function on its own right, having the required symmetry

$$\begin{aligned}\alpha(-\omega^*)&=\sqrt{(-\omega^*)^2+\mathrm{i}(-\omega^*)\nu}\\&=\sqrt{(\omega^2+\mathrm{i}\omega\nu)^*}=-(\sqrt{\omega^2+\mathrm{i}\omega\nu})^*=-\alpha^*(\omega).\end{aligned} \tag{C2}$$

We are now ready to establish the symmetry of the Brendel-Bormann susceptibility function $\chi(\omega)$ as follows

$$\begin{aligned}\chi(-\omega^*)&=\frac{\mathrm{i}D}{-\alpha^*(\omega)}\left(w\left(\frac{-\alpha^*(\omega)-\omega_0}{\sqrt{2}\sigma}\right)\right.\\&\quad\left.+w\left(\frac{-\alpha^*(\omega)+\omega_0}{\sqrt{2}\sigma}\right)\right)\\&=\frac{-\mathrm{i}D}{\alpha^*(\omega)}\left(w^*\left(\frac{\alpha(\omega)+\omega_0}{\sqrt{2}\sigma}\right)+w^*\left(\frac{\alpha(\omega)-\omega_0}{\sqrt{2}\sigma}\right)\right)\\&=\chi^*(\omega),\end{aligned} \tag{C3}$$

and where we have also employed the symmetry of the Faddeeva function $w(-z^*)=w^*(z)$. It is furthermore observed that $\mathrm{Im}\{\alpha(\omega)\}>0$ and the symmetry (C3) is valid even when ω is real valued and $\omega\neq 0$. Hence, by evaluating the function $\chi(\omega)$ at the real line we obtain the required symmetry $\chi(-\omega)=\chi^*(\omega)$ for $\omega\neq 0$ indicating that the impulse response is a real valued function which can be defined by the inverse Fourier integral

$$\chi(t)=\frac{1}{2\pi}\int_{-\infty}^{\infty}\chi(\omega)\mathrm{e}^{-\mathrm{i}\omega t}\mathrm{d}\omega. \tag{C4}$$

Due to the asymptotics established in Eq. (53) we can see that the integral defined in Eq. (C4) is absolutely integrable even though there is a weak (square root) singularity at $\omega=0$.

[1] H. M. Nussenzveig, *Causality and Dispersion Relations* (Academic Press, London, 1972).

[2] A. H. Zemanian, *Distribution Theory and Transform Analysis: An Introduction to Generalized Functions, with Applications* (McGraw-Hill, New York, 1965).

[3] R. M. Fano, Theoretical limitations on the broadband matching of arbitrary impedances, J. Franklin Inst. **249**, 57 (1950).

[4] M. Nedic, C. Ehrenborg, Y. Ivanenko, A. Ludvig-Osipov, S. Nordebo, A. Luger, B. L. G. Jonsson, D. Sjöberg, and M. Gustafsson, in *Advances in Mathematical Methods for Electromagnetics,* edited by K. Kobayashi and P. Smith (IET, London, 2020), pp. 491–514.

[5] I. S. Kac and M. G. Krein, R-functions - Analytic functions mapping the upper halfplane into itself, Am. Math. Soc. Transl. **103**, 1 (1974).

[6] N. I. Akhiezer, *The Classical Moment Problem* (Oliver and Boyd, Edinburgh, 1965).

[7] F. Gesztesy and E. Tsekanovskii, On matrix-valued Herglotz functions, Math. Nachr. **218**, 61 (2000).

[8] A. Bernland, A. Luger, and M. Gustafsson, Sum rules and constraints on passive systems, J. Phys. A **44**, 145205 (2011).

[9] M. Štumpf and S. Nordebo, Time-domain physical limitations on the response of a class of time-invariant systems, IEEE Trans. Antennas Propagat. **72**, 5110 (2024).

[10] M. Štumpf and S. Nordebo, Physical bounds on the time-domain response of a linear time-invariant system, IEEE Signal Process. Lett. **31**, 1324 (2024).

[11] N. M. Lawandy, Localized surface plasmon singularities in amplifying media, Appl. Phys. Lett. **85**, 5040 (2004).

[12] Y. Ivanenko, M. Nedic, M. Gustafsson, B. Jonsson, A. Luger, and S. Nordebo, Quasi-herglotz functions and convex optimization, R. Soc. Open Sci. **7**, 191541 (2020).

[13] C. A. Valagiannopoulos, F. Monticone, and A. Alù, PT-symmetric planar devices for field transformation and imaging, J. Opt. **18**, 044028 (2016).

[14] C. Valagiannopoulos and S. A. Tretyakov, Stability of active photonic metasurface pairs, New J. Phys. **23**, 113045 (2021).

[15] Z. Hayran and F. Monticone, Beyond the Rozanov bound on electromagnetic absorption via periodic temporal modulations, Phys. Rev. Appl. **21**, 044007 (2024).

[16] F. Monticone and A. Alú, Do cloaked objects really scatter less? Phys. Rev. X **3**, 041005 (2013).

[17] M. Štumpf and G. Antonini, Lightning-induced voltages on transmission lines over a lossy ground–an analytical coupling model based on the Cooray-Rubinstein formula, IEEE Trans. Electromagn. Compat. **62**, 155 (2019).

[18] M. Štumpf and A. T. de Hoop, Loop-to-loop pulsed electromagnetic signal transfer across a thin metal screen with Drude-type dispersive behavior, IEEE Trans. Electromagn. Compat. **60**, 885 (2017).

[19] I. E. Lager, A. T. de Hoop, and T. Kikkawa, Model pulses for performance prediction of digital microelectronic systems, IEEE Trans. Compon. Packag. Manuf. **2**, 1859 (2012).

[20] R. Brendel and D. Bormann, An infrared dielectric function model for amorphous solids, J. Appl. Phys. **71**, 1 (1992).

[21] A. D. Rakic, A. B. Djurisic, J. M. Elazar, and M. L. Majewski, Optical properties of metallic films for vertical-cavity optoelectronic devices, Appl. Opt. **37**, 5271 (1998).

[22] J. Orosco and C. F. M. Coimbra, Optical response of thin amorphous films to infrared radiation, Phys. Rev. B **97**, 094301 (2018).

[23] J. Orosco and C. F. M. Coimbra, On a causal dispersion model for the optical properties of metals, Appl. Opt. **57**, 5333 (2018).

[24] S. Nordebo, G. Kristensson, M. Mirmoosa, and S. Tretyakov, Optimal plasmonic multipole resonances of a sphere in lossy media, Phys. Rev. B **99**, 054301 (2019).

[25] Y. Mirzaei, G. Rostami, M. Dolatyari, and A. Rostami, Investigation of efficient mathematical permittivity modeling for modal analysis of plasmonics layered structures, Optik **126**, 323 (2015).

[26] A. R. Sarhan, B. B. Yousif, N. F. F. Areed, and S. S. A. Obaya, Modeling of fiber optic gold SPR sensor using different dielectric function models: A comparative study, Plasmonics **15**, 1699 (2020).

[27] E. Bailly, K. Chevrier, C. R. P. de la Vega, J.-P. Hugonin, Y. D. Wilde, V. Krachmalnicoff, B. Vest, and J.-J. Greffet, Method to measure the refractive index for photoluminescence modelling, Opt. Mater. Express **12**, 2772 (2022).

[28] F. Firouzi and S. K. Sadrnezhaad, Revisiting the experimental dielectric function datasets of gold in accordance with the Brendel-Bormann model, J. Mod. Opt. **70**, 243 (2023).

[29] N. Herguedas and E. Carretero, Optical properties in mid-infrared range of silicon oxide thin films with different stoichiometries, Nanomaterials **13**, 2749 (2023).

[30] R. L. Olmon, B. Slovick, T. W. Johnson, D. Shelton, S.-H. Oh, G. D. Boreman, and M. B. Raschke, Optical dielectric function of gold, Phys. Rev. B **86**, 235147 (2012).

[31] F. W. J. Olver, *Asymptotics and Special Functions* (A. K. Peters, Ltd, Natick, Massachusetts, 1997).

[32] M. Gustafsson and D. Sjöberg, Sum rules and physical bounds on passive metamaterials, New J. Phys. **12**, 043046 (2010).

[33] B. H. Armstrong, Spectrum line profiles: The Voigt function, J. Quant. Spectrosc. Radiat. Transfer **7**, 61 (1967).

[34] J. Humlíček, Optimized computation of the Voigt and complex probability functions, J. Quant. Spectrosc. Radiat. Transfer **27**, 437 (1982).

[35] K. Imai, M. Suzuki, and C. Takahashi, Evaluation of Voigt algorithms for the ISS/JEM/SMILES L2 data processing system, Adv. Space Res. **45**, 669 (2010).

[36] M. Kuntz, A new implementation of the Humlicek algorithm for the calculation of the Voigt profile function, J. Quant. Spectrosc. Radiat. Transfer **57**, 819 (1997).

[37] F. Schreier, Optimized implementations of rational approximations for the Voigt and complex error function, J. Quant. Spectrosc. Radiat. Transfer **112**, 1010 (2011).

[38] K. L. Letchworth and D. C. Benner, Rapid and accurate calculation of the Voigt function, J. Quant. Spectrosc. Radiat. Transfer **107**, 173 (2007).

[39] S. M. Abrarov and B. M. Quine, Efficient algorithmic implementation of the Voigt/complex error function based on exponential series approximation, Appl. Math. Comput. **218**, 1894 (2011).

[40] S. Nordebo, Uniform error bounds for fast calculation of approximate Voigt profiles, J. Quant. Spectrosc. Radiat. Transfer **270**, 107715 (2021).

[41] J. Tennyson *et al.*, Recommended isolated-line profile for representing high-resolution spectroscopic transitions (IUPAC Technical Report), Pure Appl. Chem. **86**, 1931 (2014).

[42] F. W. J. Olver, D. W. Lozier, R. F. Boisvert, and C. W. Clark, *NIST Handbook of Mathematical Functions* (Cambridge University Press, New York, 2010).

[43] M. Abramowitz and I. A. Stegun, *Handbook of Mathematical Functions*, Applied Mathematics Series Vol. 55 (National Bureau of Standards, Washington DC, 1970).

[44] R. Kress, *Linear Integral Equations*, 2nd ed. (Springer-Verlag, Berlin, 1999).

[45] J. J. Sakurai and J. Napolitano, *Modern Quantum Mechanics* (Pearson Education, Hoboken, NJ, 2011).

[46] C. F. Bohren and D. R. Huffman, *Absorption and Scattering of Light by Small Particles* (Wiley, New York, 1983).

[47] G. Kristensson, *Scattering of Electromagnetic Waves by Obstacles* (SciTech Publishing, Edison, NJ, 2016).

[48] A. Papoulis, *The Fourier Integral and its Applications* (McGraw-Hill,New York, 1962).